Endocrinology. First published ahead of print November 26, 2007 as doi:10.1210/en.2007-0814

Glucocorticoid receptor is required for skin barrier competence

Short title: Glucocorticoid receptor regulates skin development

Pilar Bayo [(1)], Ana Sanchis [(1)], Ana Bravo [(2)], Jose Luis Cascallana [(2)], Katrin Buder [(3)], Jan Tuckermann [(3,4)], Günther Schütz [(4)] and Paloma Pérez [(1,5,*)]

[(1)] Centro de Investigación Príncipe Felipe CIPF, Av. Autopista del Saler 16, Camino de las Moreras, E-46013 Valencia, Spain

[(2)] Department of Veterinary Clinical Sciences, Veterinary Faculty, University of Santiago de Compostela, E-27002 Lugo, Spain

[(3)] Molecular Biology of Tissue specific Hormone Action, Leibniz Institute for Age Research, Fritz Lipmann Institute, Beutenbergstr. 11, D-07745 Jena, Germany

[(4)] Dept. Molecular Biology of the Cell I, German Cancer Research Center, D-69120 Heidelberg, Germany

[(5)] Instituto de Biomedicina de Valencia IBV-CSIC, Jaime Roig 11, E-46010 Valencia, Spain

* Corresponding author: Paloma Pérez. Centro de Investigación Príncipe Felipe (CIPF) and Instituto de Biomedicina de Valencia (CSIC)

Address correspondence: Paloma Pérez, Centro de Investigación Príncipe Felipe, Valencia, Av. Autopista del Saler 16, Camino de las Moreras, E-46013-Valencia, Spain.

Tel +34 96 328 9680

Fax +34 96 328 9701

pperez@cipf.es

Keywords: glucocorticoid receptor, DNA-binding function, epidermal homeostasis, cross-talk, ERK

This work was supported by grant SAF2005-00412 from the Spanish Ministerio de Educación y Ciencia, by the "Fonds der Chemischen Industrie" and the European Union through grant LSHM-CT-2005-018652 (CRESCENDO) and by grant DFG Tu-220/3 from the Deutsche Forschungsgemeinschaft.

Disclosure statement: The authors of this manuscript have nothing to disclose.

Abstract

To investigate the contribution of the glucocorticoid receptor (GR) in skin development and the mechanisms underlying this function, we have analyzed two mouse models in which GR has been functionally inactivated: the knock-out $GR^{-/-}$ mice and the dimerization mutant $GR^{dim/dim}$ that mediates defective DNA binding-dependent transcription. Since GR null mice die perinatally, we evaluated skin architecture of late embryos by histological, immunohistochemical and electron microscopy studies. Loss-of-function of GR resulted in incomplete epidermal stratification with dramatically abnormal differentiation of $GR^{-/-}$, but not $GR^{+/-}$ embryos, as demonstrated by the lack of loricrin, filaggrin and involucrin markers. Skin sections of $GR^{-/-}$ embryos revealed edematous basal and lower spinous cells and electron micrographs showed increased intercellular spaces between keratinocytes and reduced number of desmosomes. The absent terminal differentiation in $GR^{-/-}$ embryos correlated with an impaired activation of caspase-14, which is required for the processing of profilaggrin into filaggrin at late embryo stages. Accordingly, the skin barrier competence was severely compromised in $GR^{-/-}$ embryos. Cultured mouse primary keratinocytes (MPK) from $GR^{-/-}$ mice formed colonies with cells of heterogeneous size and morphology that showed increased growth and apoptosis, indicating that GR regulates these processes in a cell-autonomous manner. The activity of ERK1/2 was constitutively augmented in $GR^{-/-}$ skin and MPKs relative to *wt*, which suggests that GR modulates skin homeostasis, at least partially, by antagonizing ERK function. Moreover, the epidermis of $GR^{+/dim}$ and $GR^{dim/dim}$ embryos appeared normal, thus suggesting that DNA-binding-independent actions of GR are sufficient to mediate epidermal and hair follicle development during embryogenesis.

Introduction

In mammals, the epidermis is a stratified epithelium that acts as a barrier preserving the organism from dehydration, uncontrolled thermoregulation and potentially environmental damage. The acquisition of a competent barrier occurs during embryonic development and it requires a correct balance between proliferation, differentiation and controlled apoptosis. To exert this key function, the epidermis must be able to self renew under both homeostatic and injury conditions by maintaining a population of proliferative keratinocytes in the basal layer (BL) and hair follicles (HF) (reviewed in 1, 2). The process of differentiation implies that basal keratinocytes cease to proliferate, lose adherence to the basement membrane and migrate to outer layers called spinous (SL), granular (GL) and stratum corneum (SC). During mouse skin development and, as basal cells move outwards, gene expression of basal keratinocytes, such as keratin K5, is repressed and switches towards differentiation specific markers, including keratins K1 and K10. Epidermal terminal differentiation is a tightly regulated process that ends up in the conversion of viable keratinocytes into dead, flattened squames of the SC, a process which represents a form of programmed cell death (1). In the mouse, the first suprabasal layer of the epidermis is formed around embryonic 14.5-15.5 dpc and the number of epidermal cell layers increases, with the SC being formed at 18.5 dpc. Alterations in the processes of keratinocyte proliferation and differentiation during fetal development may lead to a disturbed epidermal barrier, which can cause skin disorders of keratinization and cornification (reviewed in 3). Recent findings demonstrated that the nonapoptotic caspase-14 plays a role in epidermal homeostasis since its activation at late stages of epidermal development *in utero* is required for terminal keratinocyte differentiation, contrary to classical caspases involved in apoptosis, such as caspase-3 (4, 5).

Although glucocorticoid (GC) analogs are widely prescribed as the treatment of choice in many cutaneous disorders (6), the role of GCs in skin

development has not been completely deciphered (3). In some reports, GCs have been shown to accelerate epidermal barrier formation as seen by either GC injections *in utero* (7) or, conversely, by showing that corticotropin-releasing hormone-deficient newborn mice, which exhibited GC deficiency, had delayed maturation of the SC (8); moreover, supplementation of GCs in these mice fully rescued skin phenotype (8). In experiments performed in adult mouse skin, short-term topical and systemic GC treatment disturbed epidermal barrier competence (9). These results highlight that the responses to GCs depend on the stages in development (fetal *vs*. adult) and also due to the use of physiological *vs* pharmacological doses of GCs.

Since GC effects are mediated through the glucocorticoid receptor (GR), studying the impact of the gain- and loss-of-function of GR in skin development and function through genetically modified mice constitutes a relevant issue from the basic and clinical perspective. GR acts through the so-called genomic and non-genomic actions exerting pleiotropic roles in many tissues, including skin (reviewed in 10). GR belongs to the superfamily of steroid nuclear receptors and is a ligand-dependent transcription factor. In the absence of ligand, GR resides in the cytoplasm asociated with chaperones such as Hsp90, in an inactive form. Upon ligand binding, GR dissociates from cytoplasmic complexes, dimerizes and translocates to the nucleus, where it can then regulate gene transcription by binding to positive and negative glucocorticoid response elements (GREs). GR can regulate gene expression through DNA-binding-dependent and -independent mechanisms. The former requires ligand-induced dimerization of GR and binding to specific GREs, whereas the latter does not require DNA-binding of GR, but rather is mediated through interference with other transcription factors, such as NF-κB or AP-1 (11). Non-genomic actions of GR have been demonstrated and are mediated through physical interaction of the receptor at the plasma membrane with p85α/PI3K which, in turn, modulates AKT activity (12).

To decipher the role of GR in skin development, we have evaluated the skin architecture of two mouse models in which

GR has been functionally inactivated: the *knock-out* $GR^{-/-}$ mice (13, 14) and the *knock-in* mice carrying the point mutation A458 in the D-loop of GR, which impairs dimerization-induced DNA-binding of the GR, thus resulting in a mutant protein that display defective DNA binding-dependent transcription ($GR^{dim/dim}$, 15). $GR^{-/-}$ mice die perinatally whereas $GR^{dim/dim}$ animals are viable. Altogether, our analyses demonstrate that GR is required for proper epidermal differentiation, which is in part mediated by caspase-14 processing during mouse embryogenesis. In addition, GR regulated keratinocyte growth and apoptosis in a cell-autonomous manner, as shown by the observed increased proliferation and cell death in cultured mouse primary keratinocytes (MPKs) from $GR^{-/-}$ mice. GR controlled skin homeostasis, at least partially, through antagonistic modulation of ERK function both *in vivo* and *in vitro*. Moreover, and given that the epidermis of $GR^{dim/dim}$ embryos appeared normal, our data strongly support the idea that DNA-binding-independent actions of GR are sufficient to mediate epidermal development during embryogenesis.

Materials and methods

Animal experimentation

GR null and $GR^{dim/dim}$ mice have been previously reported (13-15). $GR^{+/-}$ hemizygous mice (C57Bl/6J) intercrosses were programmed to obtain $GR^{-/-}$, $GR^{+/-}$ and $GR^{+/+}$ mice. The same mating schedule was followed for $GR^{+/dim}$ mice to obtain $GR^{+/+}$, $GR^{+/dim}$ and $GR^{dim/dim}$ embryos. Embryos were obtained by cesarean derivation at 18.5 days post-conception (dpc; the morning of the day that the vaginal plug was seen was considered as day 0.5 pc.). Overall, we have analyzed 143 skin samples from $GR^{-/-}$, $GR^{+/-}$ and $GR^{+/+}$ embryos and 17 skin samples from $GR^{+/+}$, $GR^{+/dim}$ and $GR^{dim/dim}$ embryos. In addition, we evaluated one litter of $GR^{-/-}$, $GR^{+/-}$ and $GR^{+/+}$ 16.5 dpc embryos (n = 9). For genotyping, DNA was isolated from mouse tail and analyzed by PCR, as described (13-15). Dorsal skin was excised and either rapidly frozen in liquid nitrogen to obtain protein, fixed for immunohistochemistry or processed for preparation of mouse primary keratinocytes (MPKs).

Mice were housed in microisolated boxes in which the air is filtered in both directions, allowing maximun isolation. Animal experimentation was always conducted with accepted standards of humane animal care in our registered animal facility (CV-46007, Centro de Investigación Príncipe Felipe CIPF). Experiments were performed in accordance with the "Principles of Laboratory Animal Care" (NIH Publication no. 85-23, revised 1985) and with the current Spanish and European normative which governs research with animals (Real Decreto 1201/2005, B.O.E. #252, 10 of October, 2005 and Convenio Europeo 1-2-3 del 18/3/1986).

Antibodies

The antibodies used included rabbit polyclonal antibodies to GR (sc-1004), ERK (sc-154), JNK (sc-474), p-c-jun (sc-822), β-catenin (sc-7199), c-myc (sc-788), and caspase-14 (sc-5628) from Santa Cruz Biotechnology, Inc., (Santa Cruz, CA). Antibodies against c-jun (#9165), p-ERK (Thr202/Tyr204) (#4376) and p-JNK (Thr183/Tyr185) (#9251) were purchased from Cell Signaling (Cell Signaling Technology Inc., Beverley, MA). E-cadherin (610181), plakoglobin (610253)

and desmoglein-1 (610273) antibodies were from BD transduction Laboratories (BD Biosciences). An antibody against actin (A-2066, Sigma Chemical Co., St. Louis, MO) was used for loading control. Secondary peroxidase-conjugated anti-rabbit antibody was from Amersham (Aylesbury, UK) and secondary peroxidase-conjugated anti-mouse antibody and biotin-conjugated anti-rabbit or anti-mouse antibodies from Jackson ImmunoResearch (Jackson ImmunoResearch Laboratories, Inc. West Grove, PA).

Antibodies against keratin K5 (PRB-160P), K6 (PRB-169P), K10 (PRB-159P), loricrin (PRB-145P), filaggrin (PRB-417P) and involucrin were from Covance (Babco, Berkeley, CA).

Histological and Immunohistochemical analysis

Whole embryos and skin samples were fixed in 4% paraformaldehyde (PFA) or 70% ethanol and embedded in paraffin. Consecutive 3 to 4 μm-thick sections were obtained. For histopathology, sections were stained with hematoxylin/eosin (H&E). Prior to immunostaining, paraffin sections were dewaxed and microwaved in 10 mM citrate solution. For immunohistochemistry, paraffin sections were blocked with 5% fetal bovine serum, and then incubated with the primary antibody for at least one hour. Slides were washed three times with PBS, and then incubated with conjugated secondary antibodies for 1 h. Finally, the reaction was visualized with the Avidin-Biotin-Complex (ABC) kit from DAKO (Vectastain Elite, Vector Laboratories, Inc, Burlingame, CA) using diamino-benzidine as chromogenic substrate for peroxidase. Slides were mounted and analyzed by light microscopy (Leica DM RXA2), and microphotographs were taken at 40x magnification, unless otherwise indicated.

In vivo epidermal BrdU labeling

Epithelial cell proliferation was measured by i.p. injection of BrdU (130 μg/g of body weight, Roche) into pregnant female mice 1 h before sacrifice. BrdU incorporation was detected by immunohistochemistry of paraffin-embedded sections using a mouse anti-BrdU monoclonal antibody (biotest, Roche). The number of BrdU-positive cells and the number of total cells was

determined per 200 μm of interfollicular epithelium in each section. Experiments were performed at least in five individuals of each genotype and differences were assessed by using the t test, with statistical significance when $p < 0.05$.

Morphometric analysis

Determination of the average number of HF, HF length and epidermal width was performed using 4 μm-thick skin paraffin sections from 16.5 dpc and 18.5 dpc embryos stained with hematoxilin/eosin and counting at least 10 individual fields of 1mm per slide using the software *MetaMorph (Premier Offline 7.0, Molecular Devices)*. Experiments were performed at least in five individuals of each genotype and differences were assessed by using the t test, with statistical significance when $p < 0.05$.

Permeability barrier assays

18.5 dpc embryos were collected, euthanized and submerged in methanol for 3 min. The embryos were placed in a 0.1% solution of touidine blue dye in PBS for 2 min, washed several times in PBS, dried and photographed.

Transmission Electron Microscopy (TEM) studies

Skin samples were spread on the bottom of a 12well-plate, washed in PBS and fixed in 2.5% glutaraldehyde/2.5% PFA/PBS pH 7.2 for 15h at 20º C. Skin samples were 1 h postfixed with 1% OsO_4/PBS in the dark at 4ºC followed by dehydration in an ascending water/acetone series and embedded in AGAR 100 epoxy resin (AGAR SCIENTIFIC). The resin was allowed to polymerize for 2 days at 60º C in flat embedding moulds. Sections were obtained by an ultramicrotome (REICHERT ULTRACUT S; LEICA) and stained with 2% uranyl acetate and lead citrate at various concentrations. Sections were examined with a transmission electron microscope (CEM 902A; Zeiss) at an acceleration voltage amounted to 80 kV

MPK isolation, culture and treatments

18.5 dpc embryos were sacrificed by CO_2 asphyxiation, their bodies were rinsed in 70% ethanol and limbs and tail were

removed; tails were used for PCR genotyping. Skin was peeled off, rinsed in PBS and then incubated in 0.25% trypsin at 4ºC overnight. The epidermis was separated from dermis with forceps, minced and homogenized in complete low calcium medium by vigorous shaking 10 min at 4ºC. The filtered solution contained MPKs, which were collected by centrifugation. MPKs were pooled (two mice of each genotype) and 10^6 cells were plated into one 35 mm diameter collagen coated petri dish (BD Biosciences) and cultured at 37ºC in standard medium. After 24 h, the medium was replaced with complete low calcium medium and cells were grown until subconfluency. Cells were refed every other day. The composition of standard medium was: Essential modified Eagle´s medium EMEM (BioWhitakker, Inc., Walkersville, MD), supplemented with 4% fetal calf serum (FCS, BioWhitakker, Inc.) plus 0.6 mM Ca_2Cl and antibiotics. To prepare low-calcium medium, FCS was depleted of divalent cations by treatment with Chelex deionizing resin (BioRad, Hempstead, UK) and supplemented with Ca_2Cl to a final concentration of approximately 0.05 mM. EGF (Sigma, St. Louis, MO) (10 ng/ml) and antibiotics were added to growth medium.

Dexamethasone (Dex, Sigma, St. Louis, MO, 1 μM) or vehicle was added for the indicated times to confluent *wt* MPKs that had been incubated in charcoal-stripped serum overnight to deplete steroid hormones. Then, cells were PBS washed and either total RNA or whole cell extracts were isolated to check caspase-14 mRNA levels by semiquantitative RT-PCR using primers previously described (16) and caspase-14 and filaggrin expression by immunoblotting. Experiments were performed in triplicate and mean value ± SD estimated.

Phorbol 12-myristate 13-acetate (PMA, Sigma, St. Louis, MO) or vehicle were added to subconfluent MPKs at a final concentration of 100 ng/ml for 1 h. After this time, cells were either fixed for ERK1/2 and p-ERK1/2 immunolocalization or washed with cold PBS and then lysed to prepare whole cell extracts. Experiments were performed in triplicate and mean value ± SD estimated.

In vitro differentiation of MPKs

To assess *in vitro* differentiation, equal numbers of MPKs were plated and grown in coverslips to confluency under low calcium (0.05 mM) conditions and then shifted to high calcium (1.2 mM) for 24 h or 48 h. Differentiation of *wt* and $GR^{-/-}$ keratinocytes was assessed by phase contrast and expression of K10 and involucrin, as markers of early and late differentiation, was examined by immunofluorescence.

BrdU immunofluorescence

To determine BrdU incorporation in MPKs, cells were seeded on glass coverslips until subconfluency and then incubated with 3 µl of BrdU (biotest, Roche, 1µg/µl) for 3h at 37ºC. After fixation, cells were permeabilized, treated with HCl 2N for 30 min and then, blocked and incubated with anti-BrdU antibody (biotest, Roche) followed by anti-mouse-FITC. Coverslips were mounted with polyvinil-alcohol-DABCO (Fluka, Sigma-Aldrich Chemie, GmbH, Switzerland) containing DAPI and samples were visualized under a fluorescence microscope (Leica DM RXA2). Positive nuclei were counted (at least 500 cells, 4 coverslips per genotype) in five independent experiments and percentages of BrdU-positive cells ± SD determined. Routinely, controls of staining specificity were performed by using preimmune serum and the secondary antibodies, which gave no signal (not shown).

Analysis of apoptosis in tissue sections and cultured keratinocytes

To detect individual apoptotic cells in paraffin-embedded tissue sections and MPKs, the *In Situ Cell Death Detection kit* (Roche) was used, following manufacturer´s recommendation. Paraffin sections immersed in 0.1 M citrate buffer, pH 6 were microwave-irradiated for 5 min, and then rinsed with PBS prior to the TUNEL reaction. Four 16.5 dpc embryos of each genotype were examined.

MPKs isolated from $GR^{-/-}$ and $GR^{+/+}$ embryos (four of each genotype) were seeded on glass coverslips until subconfluency and treated as indicated. Cells were fixed and permeabilized, and incubated with the TUNEL reaction

mixture for 1 h at 37ºC in the dark. Sections were mounted with DAPI and samples visualized under a fluorescence microscope (Leica DM RXA2) to determine the percentages of apoptotic cells. As a positive control, *wt* MPKs were treated with vehicle or TNF-α (100 mg/ml) plus cycloheximide (CHX, 1 μg/ml, Sigma) for 16h, as previously described (17). When indicated, the ERK inhibitor PD098059 (50 μM, Calbiochem, San Diego, CA) was added for 16h. Quantitation of single apoptotic cells represents the mean value ± SD estimated obtained from three different experiments with MPKs using three replicates for each experimental condition. Differences were assessed by using the t test, with statistical significance when $p < 0.05$.

Immunoblotting

Whole cell extracts (20 μg) were prepared as previously described (15), boiled in Laemmli buffer and separated on 10% sodium dodecyl sulfate-polyacrylamide gels (SDS-PAGE), then transferred to nitrocellulose filters (Hybond ECL, Amersham, Aylesbury, UK). Filters were blocked with 5% nonfat dry milk in PBS-0.1% Tween 20 at 4º C overnight, washed three times in PBS-0.1% Tween 20 and incubated with the indicated antibodies. After washing, membranes were incubated with a peroxidase-conjugated secondary antibody (Amersham), washed again, and analyzed using the enhanced chemiluminiscence method (ECL, Amersham), according to manufacturer's recommendations. The membranes were also stained with Ponceau S (Sigma Chemical Co., St. Louis, MO) to verify equal protein loading and transfer.

Specific bands were scanned by using Image Quant (Amersham), quantitated with Quantity One Software (BioRad) and represented as graph bars. Values for control samples (basal protein levels in *wt* skin) were arbitrarily set as 1 and the values in $GR^{-/-}$ were expressed as relative to *wt*. Experiments were performed at least in three individuals of each genotype and differences were assessed by using the t test, with statistical significance when $p < 0.05$.

Results

GR is required for epidermal and hair follicle differentiation during embryogenesis

To investigate the consequences of GR loss-of-function in skin development, we analyzed the progeny of $GR^{+/-}$ hemizygous mice intercrosses at late embryo stages. Macroscopical observation of 16.5 and 18.5 dpc embryos revealed shiny thinner skin of $GR^{-/-}$ mice, in contrast to their *wild-type* (*wt* or $GR^{+/+}$) littermates, whereas $GR^{+/-}$ pups were indistinguishable from *wt*. Skin of $GR^{-/-}$ mice was easily damaged by mechanical stress, such as forceps manipulation used for cesarean derivation. Histological analysis by H&E staining of paraffin-embedded skin sections from 16.5 and 18.5 dpc embryos revealed that the lack of GR resulted in altered skin development with incomplete epidermal stratification and dramatically abnormal differentiation (Fig. 1). The epidermis of *wt* late embryos is organized as stratified epithelia composed of a single basal cell layer and six-to eight suprabasal cell layers, including the spinous layer (SL), the granular layer (GL) containing keratohyalin granules and the outermost layer, the stratum corneum (SC). At 16.5 dpc, epidermal maturation is characterized by the appearance of the GL and SC, key to the formation of a competent skin barrier, which is established at 18.5 dpc. In sharp contrast to *wt* late embryos, 16.5 and 18.5 dpc $GR^{-/-}$ epidermis was highly immature and featured only three to four suprabasal layers with an abnormal high number of apoptotic keratinocytes (arrows) in the lower suprabasal layers (Fig. 1, compare C and F with A and D). Apoptotic keratinocytes were further identified by *TUNEL* staining in the suprabasal layers of the $GR^{-/-}$ skin sections. In contrast, *wt* skin displayed non-apoptotic cells or few scattered apoptotic cells (Fig. 1G and data not shown). Moreover, both the GL and the SC were barely detected. However, $GR^{+/-}$ skin appeared indistinguishable from *wt* (Fig. 1B, E).

We thus examined the markers of later stages of terminal differentiation filaggrin, loricrin and involucrin in 18.5 dpc embryos (Fig. 2). Filaggrin is specifically expressed in the GL of the epidermis and loricrin and involucrin constitute the major

cornified envelope precursors. Remarkably, the expression of all these markers was either residual or absent in $GR^{-/-}$ mice, in contrast to $GR^{+/-}$ and *wt* littermates (Fig. 2).

Notably, the HFs in $GR^{-/-}$ skin had a more rudimentary appearance than *wt* and heterozygous littermates. In 18.5 dpc embryo skin, K6 was expressed at the inner root sheath of HF but absent in the interfollicular epidermis in $GR^{+/+}$ and $GR^{+/-}$, however, it was partially lost in $GR^{-/-}$ HFs, suggesting delayed differentiation (Fig. 2). We next quantitated the number of anagenic HF as well as HF length in dorsal skin of $GR^{-/-}$, $GR^{+/-}$ and $GR^{+/+}$ mice by morphometric analysis (Table 1). Surprisingly, neither the density nor the average length of HF was significantly changed, as assessed by H&E staining (Table 1).

We also performed electron microscopy studies of $GR^{+/+}$ and $GR^{-/-}$ 18.5 dpc epidermis (Fig. 3A-F) and found an abnormal morphology of keratinocytes in the BL, as well as abnormally differentiated suprabasal keratinocytes. Remarkably, the GL and SC were poorly differentiated and intercellular spaces were increased in $GR^{-/-}$ epidermis (Fig. 3B, asterisks). Keratohyalin granules appeared rudimentary with decreased electron density (Fig. 3D, arrows, compare with C) and the SC showed parakeratotic squames with increased electron density and contained cellular debris, a feature of incomplete cellular death (Fig. 3D asterisks, compare with C). Desmosomes (indicated by arrows) could be detected in all epidermal layers of $GR^{+/+}$ mice (Fig. 3E), whereas only few desmosome-like structures could be located in suprabasal layers of $GR^{-/-}$ embryo skin (Fig. 3F). Given that epidermal terminal differentiation was severely impaired in $GR^{-/-}$ mice, we evaluated the functionality of the permeability barrier in 18.5 dpc embryos by toluidine blue staining (Fig. 3G). As expected, epidermal maturation was complete in *wt* embryos at this stage and, consequently, epidermal regions that have acquired barrier appeared as white. In contrast, some regions around the paws, forelimbs, chin and neck of $GR^{-/-}$ embryos were visualized as blue, thus evidencing a compromised skin barrier function (Fig. 3G). Overall, our results indicate that GR is required for keratinocyte terminal

differentiation and thus, skin barrier competence, during embryogenesis.

Since processing of procaspase-14 seems to precede the final steps of keratinocyte differentiation (5), we investigated whether its activation was altered in GR null mice. According to previous reports, caspase-14 cleavage, represented by the large subunit p20, was already detected in 16.5 dpc *wt* epidermis although increased processing was observed in 18.5 dpc skin (Fig. 4A, upper panel). This correlated with the appearance of mature filaggrin at 16.5 and 18.5 dpc, as detected by immunoblotting (Fig. 4A, lower panel, arrowhead). Unprocessed and incompletely processed profilaggrin is indicated by a bracket. In contrast, caspase-14 processing was not detected in 16.5 dpc or 18.5 dpc GR null epidermises with undetectable levels of filaggrin at 16.5 dpc and only minor levels at 18.5 dpc (Fig. 4A). In addition, caspase-3 was not activated during fetal epidermis development in *wt* or GR null mice (Fig. 4B).

In order to determine whether the caspase-14 expression and/or processing was directly regulated by ligand-activated GR, we examined the effect of the GC analog dexamethasone (Dex) on the mRNA and protein levels of procaspase 14 in *wt* mouse primary keratinocytes (MPKs) (Fig. 4C-E). Our results showed that Dex, at a concentration inducing MPK differentiation, produced a two-fold increase in the procaspase-14 protein levels without eliciting its processing (Fig. 4D). We also checked whether Dex regulated caspase-14 at the mRNA level and found no differences in caspase-14A and -14B transcripts (Fig. 4E). In agreement with this, both caspase-14 mRNA forms were similar in $GR^{-/-}$ skin as compared to $GR^{+/+}$ (Fig. 4E).

GR inhibits keratinocyte growth in a cell-autonomous manner.

The high immaturity of $GR^{-/-}$ epidermis suggested a defective switch between proliferation and differentiation. We observed that immunolocalization of K5, normally restricted to the proliferative single BL (Fig. 5A, arrows), was abnormally found in suprabasal layers of $GR^{-/-}$ skin (Fig. 5B, arrowheads). This finding prompted us to examine whether

these K5-positive keratinocytes were indeed proliferating by assessing *in vivo* BrdU incorporation (Fig. 5C-E). In contrast to control mouse skin, in which all positive nuclei were located in the epidermal BL or in the outer root sheath of HFs (Fig. 5C, thin and thick arrow, respectively), we observed some BrdU-positive cells in the first suprabasal layer of GR null skin (Fig. 5D, arrowheads), a typical feature of hyperproliferative skin disorders. However, and despite abnormal localization of proliferating keratinocytes, we did not find statistically significant changes in the proliferation of interfollicular $GR^{-/-}$ keratinocytes as compared with *wt* epidermis (Fig. 5E, 15.3% *vs* 10.8%; $p > 0.05$). These findings were somehow unexpected since we and others previously reported that overexpression of GR exerts an anti-proliferative role in keratinocytes *in vivo* (18, 19).

In an attempt to understand this apparent contradiction and to discriminate whether GR affects keratinocyte proliferation in a cell-autonomous manner, we isolated and cultured MPKs from 18.5 dpc $GR^{-/-}$, $GR^{+/-}$ and $GR^{+/+}$ embryos. As mentioned, skin of $GR^{-/-}$ mice was thinner than that of their *wt* littermates and, accordingly, we found a reduction in the total yield of MPKs obtained from $GR^{-/-}$ as compared to $GR^{+/+}$ epidermis, which was statistically significant (1.02×10^6 cells ± 0.5 *vs* 1.80×10^6 cells ± 0.8; $n = 70$; $p < 0.05$). After plating in low-calcium medium, the number of non-adherent cells found in $GR^{-/-}$ MPKs was higher than in $GR^{+/+}$ epidermis (not shown). At day 3 after seeding, $GR^{+/+}$ and $GR^{+/-}$ MPKs had reached subconfluency and appeared as undifferentiated cells (Fig. 5F and data not shown). In sharp contrast, $GR^{-/-}$ keratinocytes formed colonies, consisting of cells with heterogeneous size and morphology, where bigger cells were located at the borders (Fig. 5F, thin arrows) and smaller rounded cells at the center (Fig. 5F, thick arrows), with many cells exhibiting apoptotic features (Fig. 5F, arrowheads; see also Fig. 8).

When cell growth was assessed in MPKs (Fig. 5G), we found a robust increase (28,12%) in the proliferation rate of $GR^{-/-}$ cells as compared with *wt* keratinocytes (12,47%). Collectively, and

despite $GR^{-/-}$ epidermis showed no overall changes in proliferation, our data indicate that GR regulates keratinocyte growth in a cell-autonomous manner.

In vitro differentiation of $GR^{-/-}$ keratinocytes

The lack of differentiation of $GR^{-/-}$ keratinocytes *in vivo* (Figs. 1-3) could be due to an intrinsic defect of these cells or to an inappropriate calcium supply, which is required for normal differentiation of keratinocytes. To examine this, we cultured MPKs isolated from $GR^{-/-}$ and *wt* littermates and analyzed their responses to an elevated concentration of calcium (Fig. 6). As reported (20), high calcium induced evident changes in *wt* keratinocyte morphology, that appeared as flat and enlarged cells, with numerous cell-cell contacts and formed epithelial sheets as differentiation proceeded (Fig. 6, $GR^{+/+}$ Ca^{2+} 24 h, 48 h). Surprisingly, the presence of high calcium in $GR^{-/-}$ MPKs caused similar morphological changes as compared to *wt* keratinocytes. Moreover, the augmented expression of keratins that are markers of differentiation, normally induced in *wt* MPKs by high calcium treatment, was similarly induced in cultured $GR^{-/-}$ keratinocytes (Fig. 6). Given that epidermal differentiation is severely impaired in $GR^{-/-}$ embryos (Fig. 1-3) but cultured $GR^{-/-}$ keratinocytes differentiate upon high calcium, our data suggest that a defect in the formation of the calcium stimulatory system of $GR^{-/-}$ skin exists, that can be overcome in cell culture by adding calcium.

Contribution of ERK to the impaired keratinocyte function of $GR^{-/-}$ mice

Given the key role of MAPKs in keratinocyte proliferation (21) and differentiation and since GR negatively regulates their function (22), we investigated MAPKs expression and function in GR null skin by immunoblotting and immunostaining. We first checked the expression of total protein and phosphorylated (p-) isoforms of the extracellular signal-regulated kinase 1/2 (ERK1/2) and c-jun-N-terminal kinase (JNK) in $GR^{+/+}$ and $GR^{-/-}$ skin from 18.5 dpc embryos (Fig. 7). Despite ERK1/2 protein levels being unaltered, p-ERK1/2 (Thr202/Tyr204, which leads to its

activation) was increased an average 3.5-fold in $GR^{-/-}$ skin as compared to controls (Fig. 7B). Immunostaining showed a marked augment of both cytosolic and nuclear p-ERK staining in $GR^{-/-}$ epidermal keratinocytes (Fig. 7C, p-ERK). In contrast to control epidermis, where p-ERK predominantly localized to GL nuclei, p-ERK was detected throughout all suprabasal layers. However, JNK and p-JNK protein levels were unchanged in GR-deficient skin with no major changes in their cellular distribution (Fig. 7A, C). Moreover, phosphorylation of c-jun on residues S63/S73 as well as total c-jun protein levels remained unchanged in $GR^{-/-}$ epidermis relative to *wt* (Fig. 7A, C).

We next used immunofluorescence staining to examine ERK activation in normally growing keratinocytes obtained from $GR^{-/-}$ and $GR^{+/+}$ mice. In *wt* keratinocytes, total ERK was predominantly localized in the cytoplasm whereas anti–p-ERK gave only weak staining above background (Fig. 8A, $GR^{+/+}$). In $GR^{-/-}$ MPKs, expression of total ERK was similar than in controls, however, the majority of cells showed a positive nuclear signal for p-ERK (Fig. 8A, $GR^{-/-}$). The enhanced activation of ERK in cultured keratinocytes from $GR^{-/-}$ mice under non stimulated conditions was confirmed by immunoblotting using whole cell extracts (Fig. 8B). Quantitation of specific bands revealed an average 3.2-fold increase of p-ERK levels in $GR^{-/-}$ MPKs as compared to *wt* keratinocytes. When MPKs were treated with PMA, a known inducer of ERK activity, we observed a similar increase of p-ERK in both $GR^{+/+}$ and $GR^{-/-}$ MPKs (Fig. 8C). Collectively, our data support a key role for GR in controlling keratinocyte function through inhibition of the MAPK/AP-1 signaling pathway.

To further demonstrate the contribution of ERK activation in the impaired keratinocyte function of $GR^{-/-}$ mice, we analyzed the apoptotic rate of cultured keratinocytes and the consequences of adding the pharmacological ERK inhibitor PD098059, which has been used extensively as selective inhibitor of the activation of the ERK-1/2 kinase, MEK-1, to block ERK-1/2 phosphorylation and activation in keratinocytes and other cell types (23, 24).

Cultured keratinoctes were grown in the absence or presence of PD098059 (50 μM) and apoptosis was evaluated by TUNEL immunostaining in *wt* and $GR^{-/-}$ MPKs, and quantitated (Fig. 8D). Basal apoptotic rate in *wt* keratinocytes (6%) was reduced in the presence of PD98059 (3%). In contrast to control cells, $GR^{-/-}$ MPKs exhibited an increase of apoptosis of approximately 16%. Moreover, inhibition of ERK reduced the augmented apoptosis of $GR^{-/-}$ keratinocytes (10%). As a positive control for apoptosis, we treated *wt* keratinocytes with TNF-α plus CHX for 16h, which augmented apoptosis approximately by six-fold (30%). Our results with pharmacological inhibitors of ERK activity provide evidences that the increased apoptosis rate in $GR^{-/-}$ keratinocytes is, at least partially, linked to augmented ERK activation in these cells, in agreement with previous reports (25).

To further investigate the mechanisms underlying GR function in skin development, we used $GR^{dim/dim}$ mice carrying a point mutation that impairs dimerization-induced DNA-binding of the GR (15). Our histological analysis revealed no differences between $GR^{dim/dim}$, $GR^{+/dim}$ and *wt* littermates either in epidermal or HF formation (Fig. 9A). In addition, we found no differences in the expression and localization of the markers of keratinocyte proliferation and differentiation K5, K10 and loricrin (Fig. 9B). Collectively, data obtained from the analysis of $GR^{dim/dim}$ embryos along with those regarding the role of ERK in $GR^{-/-}$ skin support the idea that GR regulates epidermal formation during embryogenesis most likely through DNA binding-independent actions.

Discussion

Role of GR in epidermal proliferation and differentiation

Although skin serves additional functions, its primary purpose is to form a protective barrier to harmful environmental stimuli. The epidermis is a squamous stratified epithelium that matures following through complex processes involving a correct balance between proliferation, differentiation and apoptosis. However, the mechanisms of stratification and, in particular, the effects of GC action on skin development are still poorly understood (3). We previously reported that overexpression of GR in epidermal basal cells by means of the K5 promoter (K5-GR mice) produced strong epidermal hypoplasia and dysplastic HFs during skin development (18, 26). However, the impact of GR loss-of-function in skin development had remained unexplored until now. In the present work, we demonstrate that $GR^{-/-}$ skin, but not $GR^{dim/dim}$, featured a highly disorganized architecture with incomplete epidermal stratification and cornification defined by the lack of terminal differentiation (Figs. 1-4 and 8). Although many key processes that are impaired in the $GR^{dim/dim}$ mice (15, 27) are most likely due to defective DNA binding-dependent transactivation of GR, neither A458T nor other GR dimerization mutants are globally deficient in transactivating via GR at promoters, as demonstrated by several reports (28, 29). This implies that the mechanisms through which GR controls keratinocyte function could depend on nontranscriptional events, on transrepression, or on transactivation of genes with a more complex GRE configuration, that can be regulated in the $GR^{dim/dim}$ mice, as occurs with PNMT gene (28, 29).

Skin barrier acquisition starts at 16.5 dpc on the dorsal surface and spreads laterally to the ventral surface in a patterned fashion (3). Our present findings demonstrate that GR is required for epidermal terminal differentiation and skin barrier function (Figs. 1-3). However, cultured $GR^{-/-}$ MPKs differentiated *in vitro* upon high calcium, thus supporting the hypothesis that a defect in the formation of the calcium stimulatory system of $GR^{-/-}$ skin exists, that can be overcome in cell culture by adding calcium.

A recent report has identified the transcriptomic profile of cultured human keratinocytes in response to GCs (19). In this work, the authors propose that GCs may have a dual effect on epidermal differentiation by promoting the late stages of terminal differentiation and, at the same time, inhibiting the early stages. In particular, several genes encoding for enzymes involved in SC formation were identified as GC-regulated, such as transglutaminase 1, filaggrin and corneodesmosin (19). These findings are in agreement with our *in vivo* model.

On the other hand, the ultrastructure of $GR^{-/-}$ embryo skin featured revealed a reduced number of desmosomes (Fig. 3). Previous reports indicated that GCs up-regulate several adhesion molecules, including markers of adherens junctions (E-cadherin), desmosomes (desmoglein-1) or both (plakoglobin)(19). We examined the expression of these markers in GR-deficient skin and found reduced levels of these molecules as compared to controls (not shown).

Remarkably, GR knock-out embryos exhibit increased levels of ACTH and corticosterone as a compensatory mechanism for the GR loss-of function (13). Our results indicate that excess steroid hormones rather correlate with defective epidermal maturation than cause these defects. Accordingly, impaired proliferation and apoptosis as well as constitutively augmented ERK activity was found in $GR^{-/-}$ keratinocytes, which suggests that the observed effects are independent of increased hormone levels.

Another relevant finding of this study reveals that GR loss-of-function correlates with the lack of processing of caspase-14, which prevents the formation of mature filaggrin and thus, the appearance of SC providing mammals with a competent epidermal barrier function. Our results show that ligand-activated GR regulates caspase-14 expression in cultured keratinocytes at the post-transcriptional level. The effect of Dex on caspase-14 expression occurred at concentrations inducing keratinocyte differentiation. Noteworthy, the regulation of caspase-14 *in vivo* was also post-transcriptional since no changes in caspase-14 transcripts were found in $GR^{-/-}$ skin as compared to $GR^{+/+}$

mice (Fig. 4). The importance of caspase-14 as a GR target is supported by the recent findings in caspase-$14^{-/-}$ mice. These mice exhibited reduced skin-hydration levels and increased water loss and an altered profilaggrin processing pattern that could explain the observed phenotype (30). However, other proteolytic enzymes of this family, such as caspase-1 and -4 have been described as GC-targets in keratinocytes (19).

Remarkably, and despite the reported anti-proliferative role of GR, GR null mice did not show overall increased epidermal proliferation *in vivo* (Fig. 5). However, we observed abnormal proliferating suprabasal keratinocytes in $GR^{-/-}$ skin that indicated a defective switch between proliferation and differentiation. When MPKs were cultured, an increased proliferation rate of $GR^{-/-}$ keratinocytes as compared to *wt* was apparent (Fig. 5), thus demonstrating that GR regulates keratinocyte proliferation in a cell-autonomous manner.

GR modulates ERK activity to regulate keratinocyte function

Since MAPK/AP-1 signaling pathway plays a relevant role in keratinocyte biology (reviewed in 31), and given that GR inhibits MAPK function in several cell types, we analyzed whether ERK and JNK activities were altered in GR-deficient keratinocytes. We found an increase in p-ERK1/2 but not JNK activity in $GR^{-/-}$ keratinocytes by immunoblotting and immunostaining techniques (Figs. 6 and 7). It is assumed that ERK1 and ERK2 isoforms play unique roles since ERK1-deficient mice are viable whereas ERK2 knock out mice are embryonic lethal (32, 33). However, one should also consider that a threshold of total ERK activity may be required, at least in skin, since in this tissue, ERK2 cannot compensate for the loss of ERK1 (33). Given that both p-ERK1/2 isoforms were augmented in the epidermis as a consequence of GR loss-of-function, our data suggest that the hormone receptor modulates both activities. Recent work has highlighted the relevance of ERK1 in skin homeostasis and skin tumor development (25). ERK1-deficient mice showed reduced proliferation of basal keratinocytes upon TPA treatment and resistance to

development of skin papillomas induced by 7,12-dimethylbenz(a)anthracene (DMBA)-TPA protocol (25). Worth noting, the delayed tumor appearance and reduced tumor number and size found in ERK1 null mice was also reported in K5-GR transgenic mice that were subjected to different protocols of tumor formation (34, 35). Collectively, the existing data argue in favour of antagonistic functions of GR and ERK in keratinocyte proliferation.

On the other hand, ERK1 has also been implicated in modulating the proliferation/apoptosis balance, based on the increased epidermal thickness and the resistance of ERK1-deficient MPKs to apoptosis. In *wt* skin, p-ERK was predominantly localized to nuclei in the granular layer (Fig. 7), which would fit with the proposed role of ERK in keratinocyte apoptosis. In contrast, p-ERK was detected throughout all suprabasal layers in $GR^{-/-}$ skin and, remarkably, most of p-ERK staining was detected in $GR^{-/-}$ keratinocytes exhibiting apoptotic features (Fig. 7). According with this, the phenotype of MPKs from GR null mice (increased growth and apoptotic features; Figs. 5 and 8) was the opposite of that found in ERK null primary keratinocytes (reduced growth and resistance to apoptotic signals; 25). The fact that constitutive ERK activation was found in normally growing keratinocytes from $GR^{-/-}$ mice by immunofluorescence and immunoblotting (Fig. 8) further supports a role for GR in controlling ERK function. Given that $GR^{-/-}$ MPKs exhibited increased apoptosis, which was partially reduced by a selective ERK inhibitor, as demonstrated by TUNEL assays, our data reinforce that GR plays a role in keratinocyte apoptosis through regulation of the ERK function (Fig. 8D, E). Our results are in agreement with the reduced apoptosis response of $ERK^{-/-}$ keratinocytes both *in vivo* in total skin, and in culture (25).

Since the role of ERK2 has not been yet defined, it cannot be ruled out that the observed changes in this isoform modulate other aspects of keratinocyte function, such as differentiation. In this regard, previous studies in primary human keratinocytes have shown that sustained activity of ERK suppresses and ERK inhibition induces differentiation (36).

Surprisingly, we did not detect major changes in either the protein levels or cellular distribution of JNK, p-JNK, c-jun and p-c-jun in GR-deficient skin relative to *wt* (Fig. 6). This was rather unexpected given the reported negative cross-talk between GR and JNK in many cell types, including keratinocytes (11, 22). A recent work by Gazzel and coworkers has examined the transcriptomic profile of human keratinocytes upon pharmacological inhibition of the JNK pathway (37). The outcome of this study is that JNK does not directly regulate many cell-cycle and proliferation genes but rather modulates proliferation as a consequence of keratinocyte differentiation.

We previously reported that GR-mediated repression of AP-1 target genes in skin upon phorbol ester treatment occurred through the DNA binding-independent function of GR (38). However, and despite many AP-1 target genes in the epidermis include members of the cytokeratin gene family that are repressed by GR (22, 39), we did not observe changes in the level of these transcripts (not shown). It is feasible that GR play differential roles during epidermal development as compared to stress responses in adult individuals. Overall, our present findings demonstrate that GR is required for epidermal terminal differentiation and skin barrier competence during embryo development.

Acknowledgements

This work was supported by grant SAF2005-00412 of the Ministerio de Educacion y Ciencia from the Spanish Government, and by the "Fonds der Chemischen Industrie" and the European Union through grant LSHM-CT-2005-018652 (CRESCENDO) and by grant DFG Tu-220/3 from the Deutsche Forschungsgemeinschaft. We here declare that there is no conflict of interest of any of the participant institutions.

References

1 **Fuchs E, Raghavan S** 2002 Getting under the skin of epidermal morphogenesis. Nature Rev Genetics 3:199–209

2 **Schmidt-Ullrich R, Paus R** 2005 Molecular principles of HF induction and morphogenesis. BioEssays 27:247–261

3 **Segre JA** 2006 Epidermal barrier formation and recovery in skin disorders. J. Clin. Invest. 116:1150–1158

4 Lippens S, M Kockx, M Knaapen, L Mortier, R Polakowska, A Verheyen, M Garmyn, A Zwijsen, P Formstecher, D Huylebroeck, P Vandenabeele, Declercq W 2000 Epidermal differentiation does not involve the pro-apoptotic executioner caspases, but is associated with caspase-14 induction and processing. Cell Death and Differentiation 7:1218–1224

5 **Fischer H, Rossiter H, Ghannadan M, Jaeger K, Barresi C, Declercq W, Tschachler E, Eckhart L** 2005 Caspase-14 but not caspase-3 is processed during the development of fetal mouse epidermis. Differentiation 73:406–413

6 **Schäcke H, Döcke WD, Asadullah K** 2002 Mechanisms involved in the side effects of glucocorticoids. Pharmacology & Therapeutics 96:23–43

7 **Aszterbaum M, Feingold KR, Menon GK, Williams ML** 1993 Glucocorticoids accelerate fetal maturation of the epidermal permeability barrier in the rat J Clin Invest. 91(6):2703–2708

8 **Hanley K, Feingold KR, Komuves LG, Ellias P, Muglia LJ, Majzoub JA, Williams ML** 1998 Glucocorticoid deficiency delays stratum cornrum maturation in fetal mouse. J Invest Dermatol 11:440–444

9 **Kao JS, Fluhr JW, Man M-Q, Fowler AJ, Hachem JP, Crumrine D, Ahn SK, Brown BE, Elias PM, Feingold KR** 2003 Short-Term Glucocorticoid Treatment Compromises Both Permeability Barrier Homeostasis and Stratum Corneum Integrity: Inhibition of Epidermal Lipid Synthesis Accounts for Functional Abnormalities. J Invest Dermatol 120:456–464

10 **Lu NZ, Cidlowski JA** 2006 Glucocorticoid receptor isoforms generate transcription specificity. TRENDS in Cell Biology 16 (6) 301–307

11 **De Bosscher K, Vanden berghe W, Haegeman G** 2003 The Interplay between the Glucocorticoid Receptor and Nuclear Factor-kB or Activator Protein-1: Molecular Mechanisms for Gene Repression. Endocrine Reviews 24(4):488–522

12 **Losel R, Wehling M** 2003 Nongenomic actions of steroid hormones. Nat Rev Mol Cell Biol 4(1):465–615

13 **Cole TJ, Blendy AP, Monaghan K, Schmid W, Aguzzi A, Fantuzzi G, Hummler E, Unsicker K, Schütz G** 1995 Targeted disruption of the glucocorticoid receptor gene blocks adrenergic chromaffin cell development and severely retards lung maturation. Genes Dev 9:1608–1621

14 **Tronche F, Kellendonk C, Reichardt HM, Schütz G**. 1998 Genetic dissection of glucocorticoid receptor function in mice. Curr Opin Genet Dev 8:532–538

15 **Reichardt HM, Kaestner KH, Tuckermann J, Kretz O, Wessely O, Bock R, Gass P, Schmid W, Herrlich P, Angel P, Schütz, G**. 1998 DNA binding of the glucocorticoid receptor is not essential for survival. Cell 93:531–541

16 **Lippens S, VandenBroecke C, Van Damme1 E, Tschachler E, Vandenabeele P, Declercq W** 2003 Caspase-14 is expressed in the epidermis, the choroids plexus, the retinal pigment epithelium and thymic Hassall's bodies. Cell Death and Differentiation 10:257–259

17 **Leis H, Sanchis A, Pérez P** 2007 Deletion of the N-terminus of IKKγ induces apoptosis in keratinocytes and impairs the AKT/PTEN signaling pathway. Exp. Cell Res 313:742–752

18 **Pérez P, Page A, Bravo A, Del Río M, Gimenez-Conti I, Budunova IV, Slaga TJ, Jorcano JL** 2001 Altered skin development and impaired proliferative and inflammatory responses in transgenic mice overexpressing the glucocorticoid receptor. FASEB J 15:2030–2032

19 **Stojadinovic O, Lee B, Vouthounis C, Vukelic S, Pastar I, Blumenberg M, Brem H, Tomic-Canic M** 2007 Novel Genomic Effects of Glucocorticoids in Epidermal Keratinocytes. Inhibition of apoptosis, interferon-gamma pathway, and wound healing along with promotion of terminal differentiation. J Biol Chem 282 (6):4021–4034, 2007

20 **Hennings H, Michael D, Cheng C, Steinert P, Holbrook K, Yuspa SH** 1980 Calcium regulation of growth and differentiation of mouse epidermal cells in culture. Cell 19:245–254

21 **Shaulian E, Karin M** 2002 AP-1 as a regulator of cell life and death. Nat Cell Biol 4:E131–E136

22 **Herrlich P** 2001 Cross-talk between glucocorticoid receptor and AP-1. Oncogene 20 2465–2475

23 **Bollag WB, Zhong X, Dodd ME, Hardy DM, Zheng X, Allred WT** 2005 Phospholipase D Signaling and Extracellular Signal-Regulated Kinase-1 and -2 Phosphorylation (Activation) Are Required for Maximal Phorbol Ester-Induced Transglutaminase Activity, a Marker of Keratinocyte Differentiation. J Pharmacol Exp Ther 312(3):1223–1231

24 **Sanchez-Tillo E, Comalada M, Xaus J, Farrera C, Valledor AF, Caelles C, Lloberas J, Celada A** 2007 JNK1 Is Required for the Induction of *Mkp1* Expression in Macrophages during Proliferation and Lipopolysaccharide-dependent Activation. J Biol Chem 282(17):12566–12573

25 **Bourcier C, Jacquel A, Hess J, Peyrottes I, Angel P, Hofman P, Auberger P, Pouyssegur J, Pagès G**. 2006 p44 mitogen-activated protein kinase (extracellular signal-

regulated kinase 1)-dependent signaling contributes to epithelial skin carcinogenesis Cancer Res. 66(5):2700–2707

26 **Cascallana JL, Bravo A, Donet E, Leis H, Lara MF, Paramio JM, Jorcano JL, Pérez P** 2005 Ectoderm-Targeted Overexpression of the Glucocorticoid Receptor Induces Hypohidrotic Ectodermal Dysplasia. Endocrinology 146(6):2629–2638

27 **Tuckermann JP, Kleiman A, Moriggl R, Spanbroek R, Neumann A, Illing A, Clausen BE, Stride B, Förster I, Habenicht AJR, Reichardt HM, Tronche F, Schmid W, Schütz G** 2007 Macrophages and neutrophils are the targets for immune suppression by glucocorticoids in contact allergy. J Clin Invest 117(5):1381–1390

28 **Adams M**, **Meijer OC**, **Wang J**, **Bhargava A**, **Pearce D** 2003. Homodimerization of the glucocorticoid receptor is not essential for response element binding: activation of the phenylethanolamine N-methyltransferase gene by dimerization-defective mutants. Mol Endocrinol 17(12):2583–2592

29 **Rogatsky I, Wang JC, Derynck MK, Nonaka DF, Khodabakhsh DB, Haqq CM, Darimont BD, Garabedian MJ, Yamamoto KR 2003.** Target-specific utilization of transcriptional regulatory surfaces by the glucocorticoid receptor. P Natl Acad Sci USA. 100(24):13845–138450

30 **Denecker G, Hoste E, Gilbert B, Hochepied T, Ovaere P, Lippens S, Van den Broecke C, Van Damme P, D'Herde K, Hachem JP, Borgonie G, Presland RB, Schoonjans L, Libert C, Vandekerckhove J, Gevaert K, Vandenabeele P, Declercq W** 2007 Caspase-14 protects against epidermal UVB photodamage and water loss. Nat Cell Biol. 9(6):666–674

31 **Angel P, Szabowski1 A, Schorpp-Kistner M** 2001 Function and regulation of AP-1 subunits in skin physiology and pathology. Oncogene 20:2413–2423

32 **Pagès G**, **Guérin S**, **Grall D**, **Bonino F**, **Smith A**, **Anjuere F**, **Auberger P**, **Pouysségur J**.1999 Defective thymocyte maturation in p44 MAP kinase (Erk 1) knockout mice. Science 286:1374–1347

33 **Saba-El-Leil MK**, **Vella FD**, **Vernay B**, **Voisin L**, **Chen L**, **Labrecque N**, **Ang SL**, **Meloche S**.2003 An essential function of the mitogen-activated protein kinase Erk2 in mouse trophoblast development. EMBO Rep 4:964–968

34 **Budunova IV, Kowalczyk D, Pérez, P, Yao YJ, Jorcano JL, Slaga TJ** 2003 Glucocorticoid receptor functions as a potent suppressor of mouse skin carcinogenesis. Oncogene 22:3279–3287

35 **Leis H, Page A, Ramirez A, Bravo A, Segrelles C, Paramio J, Barettino D, Jorcano JL, Pérez P** 2004 Glucocorticoid Receptor Counteracts Tumorigenic Activity of Akt in Skin through Interference with the Phosphatidylinositol 3-Kinase Signaling Pathway. Mol Endocrinol 18(2):303–311

36 **Haase I, Hobbs RM, Romero MR, Broad S, Watt FM** 2001 A role for mitogen-activated protein kinase activation by integrins in the pathogenesis of psoriasis. J Clin Invest. 108(4):527–536

37 **Gazel A, Banno T, Walsh R, Blumenberg M** 2006 Inhibition of JNK Promotes Differentiation of Epidermal Keratinocytes J Biol Chem 281(29):20530–20541

38 **Tuckermann JP, Reichardt HM, Arribas R, Richter KH, Schütz G, Angel P** 1999 The DNA-binding-independent function of the glucocorticoid receptor mediates repression of AP-1-dependent genes in skin. J Cell Biol 147:1365–1370

39 **Radoja N, Komine M, Jho SH, Blumenberg M, Tomic-Canic M** 2000 Novel mechanism of steroid action in skin through glucocorticoid receptor monomers. Mol Cell Biol 20(12):4328–39

Figure legends

Fig. 1. Loss of GR results in immature skin with incomplete stratification and dramatically abnormal differentiation and reduced number of hair follicles in 16.5 and 18.5 dpc embryos. Histological analysis by H&E staining in paraffin-embedded skin sections revealed thinner undifferentiated skin in $GR^{-/-}$ embryos (C, F) as compared with $GR^{+/-}$ (B, E) and *wild-type* ($GR^{+/+}$) littermates (A, D). Note the thinner epidermis (double headed arrow) and the high number of apoptotic keratinocytes (arrows) in $GR^{-/-}$ embryos. Dotted line delineates the basement membrane. BL, basal layer; SL: spinous layer; GL, granular layer; SC, stratum corneum. Bars: 50 μm. (G) TUNEL staining was performed in paraffin-embedded skin sections from $GR^{+/+}$ and $GR^{-/-}$ 16.5 dpc embryos. Dashed lines delineate the basement membrane and the most outer layer of the epidermis. Non-apoptotic keratinocytes were found in $GR^{+/+}$ skin whereas numerous TUNEL-positive apoptotic keratinocytes (arrows) were detected in the lower suprabasal layers of $GR^{-/-}$ epidermis.

Fig. 2. Lack of terminal differentiation and abnormal HF differentiation in $GR^{-/-}$ epidermis. Expression of filaggrin, loricrin, involucrin and K6 was determined in paraffin-embedded dorsal skin of 18.5 dpc $GR^{-/-}$, $GR^{+/-}$ and wild-type ($GR^{+/+}$) littermates by immunostaining using specific antibodies. Arrows in $GR^{+/+}$ and $GR^{+/-}$ point to the expression of K6 at the inner root sheath of HF. Bars: 50 μm.

Fig. 3. Skin barrier competence is impaired in $GR^{-/-}$ mice. A) Differential ultrastructure of epidermis of $GR^{+/+}$ (A, C, E) and $GR^{-/-}$ (B, D, F) 18.5 dpc embryos. Electron micrographs demonstrated the presence of basal (BL) and spinous layers (SL) in both $GR^{+/+}$ and $GR^{-/-}$ epidermises; however, granular layer (GL) and the stratum corneum (SC) in $GR^{-/-}$ skin appeared poorly differentiated (B). Intercellular spaces were increased in $GR^{-/-}$ epidermis (B, asterisks). Dashed line marks the epidermal-dermal boundary. Note that in $GR^{-/-}$ skin, keratohyalin granules appeared rudimentary with decreased electron density (D, arrows) whereas SC showed increased electron density and contained cellular debris (D, asterisks). Desmosomes (E, F,

arrows) could be easily detected in $GR^{+/+}$ skin in BL, SL and GL, whereas in suprabasal layers of $GR^{-/-}$ epidermis, only few desmosome-like structures could be located (F). Bars: 20 μm (A, B, E, F), 1 μm (C, D). G) Permeability barrier in 18.5 dpc embryos, as assessed by toluidine blue staining. Epidermal maturation was complete in *wt* embryos at this stage (white) whereas some regions around the paws, forelimbs, chin and neck of $GR^{-/-}$ embryos were visualized as immature and permeable regions (blue).

Fig. 4. Caspase-14 processing and stratum corneum (SC) formation in late embryo epidermis from *wt* and $GR^{-/-}$ mice. (A) Total skin protein extracts from 16.5 dpc and 18.5 dpc embryos were subjected to immunoblotting using anti-caspase-14 and anti-filaggrin antisera. The size of molecular weight markers is indicated on the left. Procaspase-14 (p30) and the large subunit (p20) of caspase-14 are indicated by an arrow and arrowhead, respectively. Unprocessed and incompletely processed profilaggrin is indicated by a bracket and mature filaggrin is indicated by an arrowhead. (B) Caspase-14 and caspase-3 expression in 18.5 dpc epidermises from *wt* and $GR^{-/-}$ mice were analyzed by immunostaining using specific antibodies. Note that, contrary to caspase-14, caspase-3 was not detected in developing fetal mouse epidermis. Bars: 50 μm. (C) Mouse primary keratinocytes (MPKs) obtained from *wt* mice were cultured until confluency, then treated with either vehicle (-) or Dex 1 μM for 48 h to induce differentiation. Bar: 50 μm. (D) Protein lysates were prepared from vehicle- or Dex-treated MPKs as well as 16.5 dpc $GR^{-/-}$ and *wt* skin to examine caspase-14 and filaggrin expression. (E) Total RNA was isolated from vehicle- or Dex-treated MPKs and 16.5 dpc $GR^{-/-}$ and *wt* skin to check caspase-14 mRNA transcripts by RT-PCR using specific primers.

Fig. 5. Augmented keratinocyte proliferation in $GR^{-/-}$ MPKs. (A) K5 immunostaining in $GR^{+/+}$ (A) and $GR^{-/-}$ (B) skin. Epidermal proliferation was assessed in $GR^{+/+}$ (C) and $GR^{-/-}$ (D) littermates by immunostaining using an anti-BrdU antibody. All positive interfollicular keratinocytes (arrows) detected in *wt* epidermis were located in the epidermal basal layer whereas suprabasal positive nuclei (arrowhead) were also seen in $GR^{-/-}$ embryos. (E)

Quantitation of positive-BrdU cells was expressed as the percentage of total number of counterstained nuclei; $p > 0.05$; n = 11. (F) MPKs obtained from $GR^{+/+}$ and $GR^{-/-}$ littermates were cultured for 3 days. At the time of subconfluency, MPKs from $GR^{-/-}$ mice formed heterogeneous colonies with smaller rounded cells at the center (arrows) and signs of increased cell death (arrowhead). (G) BrdU incorporation was determined by immunofluorescence and quantitated. Percentage of positive-BrdU cells relative to total number of nuclei stained with DAPI was expressed; * $p < 0.0001$; n = 6. Bars: 50 μm.

Fig. 6. *In vitro* keratinocyte differentiation in $GR^{-/-}$ MPKs. Epidermal MPKs were plated and grown in coverslips to confluency under low calcium (0.05 mM) conditions and then shifted to high calcium (1.2 mM) for 24 h or 48 h, as indicated. (A) Differentiation of $GR^{+/+}$ and $GR^{-/-}$ keratinocytes was assessed by phase contrast. Bar: 50 μm. (B) Expression of K10 and involucrin, as markers of early and late differentiation, was examined by immunofluorescence. Experiments were performed in duplicate by using four mice of each genotype (n = 4). Bar: 50 μm.

Fig. 7. ERK1/2 activity is increased in 18.5 dpc $GR^{-/-}$ epidermis. (A) Immunoblotting using whole cell extracts obtained from $GR^{+/+}$ and $GR^{-/-}$ skin was performed to check expression of ERK1/2, phosphorylated (p)-ERK1/2, JNK, JNK, c-jun and p-c-jun. Actin was used as a loading control. (B) Protein levels were normalized to actin and statistically significant differences calculated. Only the ratio of p-ERK relative to total ERK was found statistically significant; * $p < 0.05$; n = 5. (C) Immunostaining of $GR^{+/+}$ and $GR^{-/-}$ skin showing localization of p-ERK, p-JNK an p-c-jun. ERK1/2 was constitutively increased in $GR^{-/-}$ epidermis. Bars: 50 μm.

Fig. 8. ERK1/2 activation in $GR^{-/-}$ MPKs contributes to increased keratinocyte apoptosis. (A) Immunofluorescence of $GR^{+/+}$ and $GR^{-/-}$ MPKs showing localization of total and p-ERK. DAPI

nuclear staining is also shown. All pictures were taken at the same magnification. Bar: 50 μm (B) Immunoblotting using whole cell extracts obtained from MPKs from $GR^{+/+}$ and $GR^{-/-}$. MPKs were checked for expression of ERK1/2 and p-ERK1/2 in the absence or presence of PMA (100 ng/ml) for 1 h. Actin was used as a loading control. (C) Quantitation of B. Protein levels were normalized to actin and the ratio of p-ERK to total ERK was calculated and found statistically significant; * $p < 0.05$; n = 6. (D) The apoptosis rate of $GR^{+/+}$ and $GR^{-/-}$ MPKs was assayed by TUNEL staining and quantitated relative to total nuclei. MPKs were grown until subconfluency and treated with either vehicle or the ERK inhibitor PD098059 (50 μM, 16 h). TNF-α (100 mg/ml) plus cycloheximide (CHX, 1 μg/ml) was added to *wt* MPKs for 16h as a positive control for apoptosis. Three different experiments using three replicates for each experimental condition were performed and differences assessed by the t test. Asterisks indicate statistically significant differences relative to *wt* MPKs, * $p < 0.0001$. Apoptotic rate of $GR^{-/-}$ MPKs treated with PD98059 also had statistical significance as compared to untreated $GR^{-/-}$ MPKs, $p < 0.001$.

Fig. 9. Normal embryonic epidermal development of $GR^{dim/dim}$ mice. (A) 18.5 dpc embryos of the indicated genotypes were analyzed by H&E staining (n = 17). Skin development was impaired in $GR^{-/-}$ mice but normal in $GR^{dim/dim}$ mice as compared with wild-type ($GR^{+/+}$) littermates. Edematous basal and lower spinous cells and high number of apoptotic keratinocytes (arrows) are indicated in $GR^{-/-}$ embryos. Bars: left panels: 100 μm; right panels: 50 μm. (B) Immunostaining in $GR^{+/+}$ and $GR^{dim/dim}$ 18.5 dpc embryo skin using specific antibodies against K5, K10 and loricrin. Bars: 50 μm.

Table 1. Morphometric analysis of 18.5 dpc $GR^{-/-}$, $GR^{+/-}$ and $GR^{+/+}$ littermates Quantitation of hair follicle (HF) number/mm and HF average length was performed in H&E dorsal skin sections, as indicated in Materials and Methods (n = 4, $p > 0.05$).

Bayo, Table 1

DORSAL SKIN	Nº HF/mm (Mean ± SD)	HF average length (μm) (Mean ± SD)
GR $^{+/+}$	9.24±1.2	89.83±3.5
GR $^{+/-}$	8.41±2.1	89.07±2.8
GR $^{-/-}$	10.8±4.8	78.64±2.4

Bayo, Fig.1

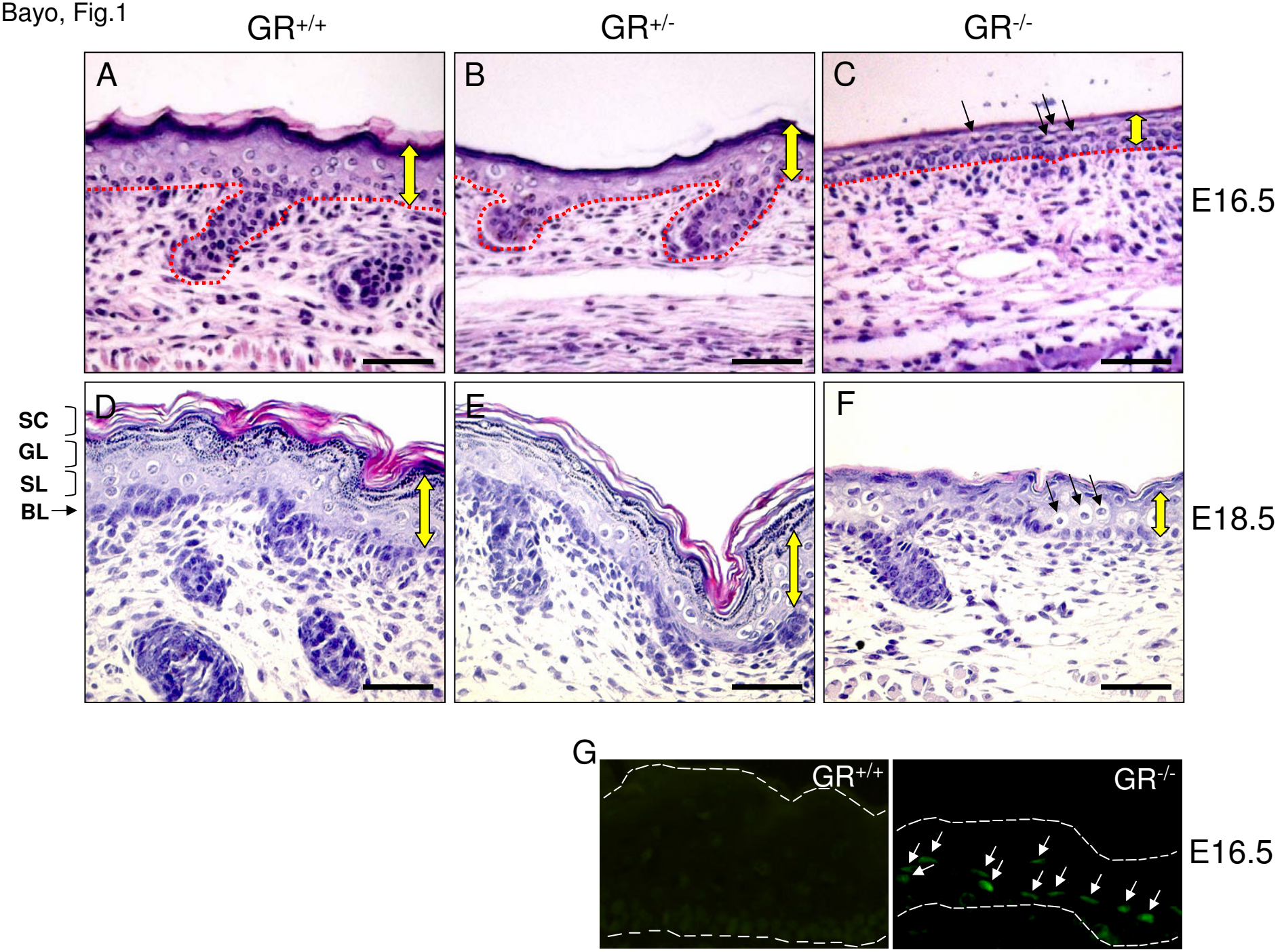

Bayo, Fig.2

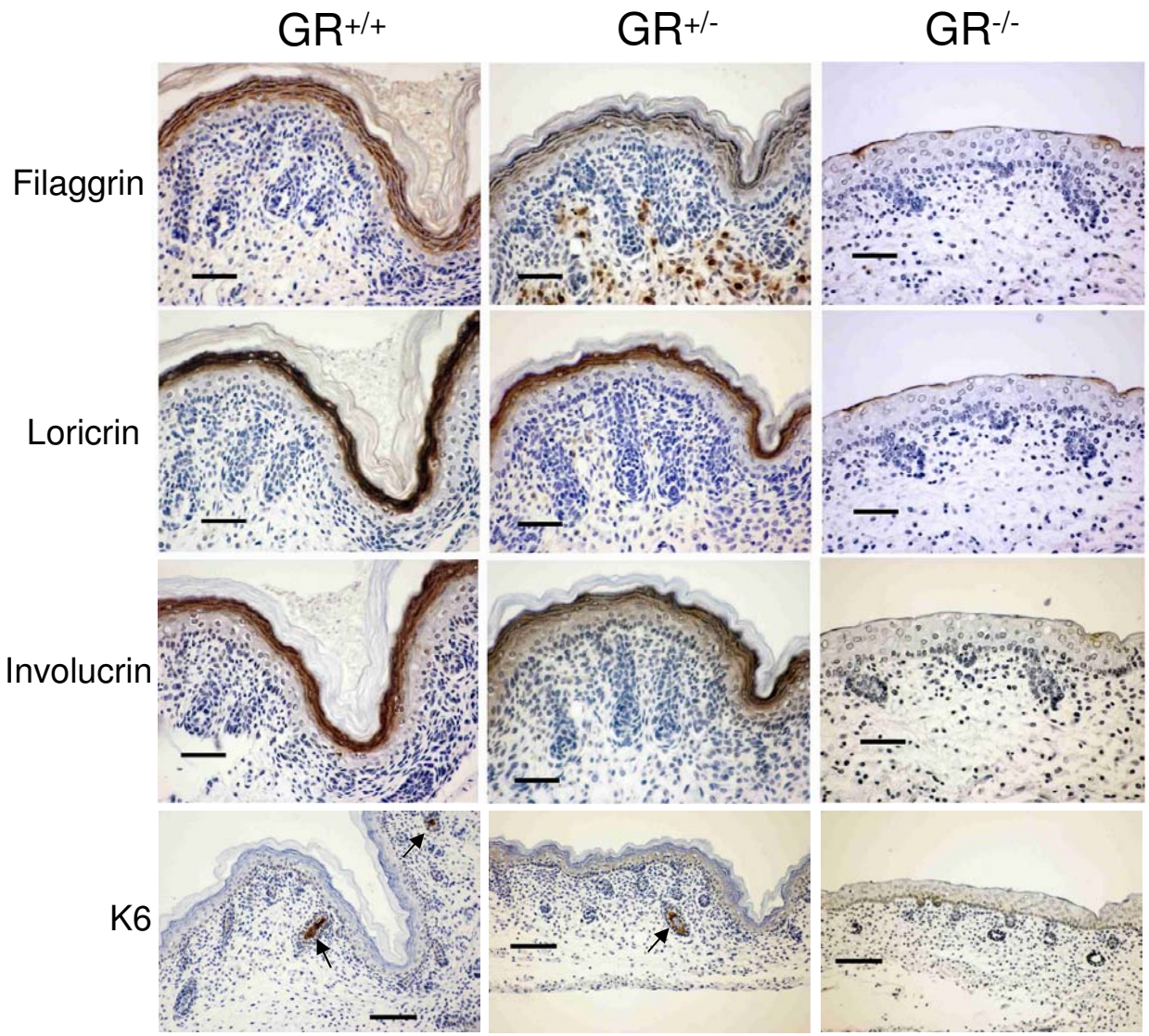

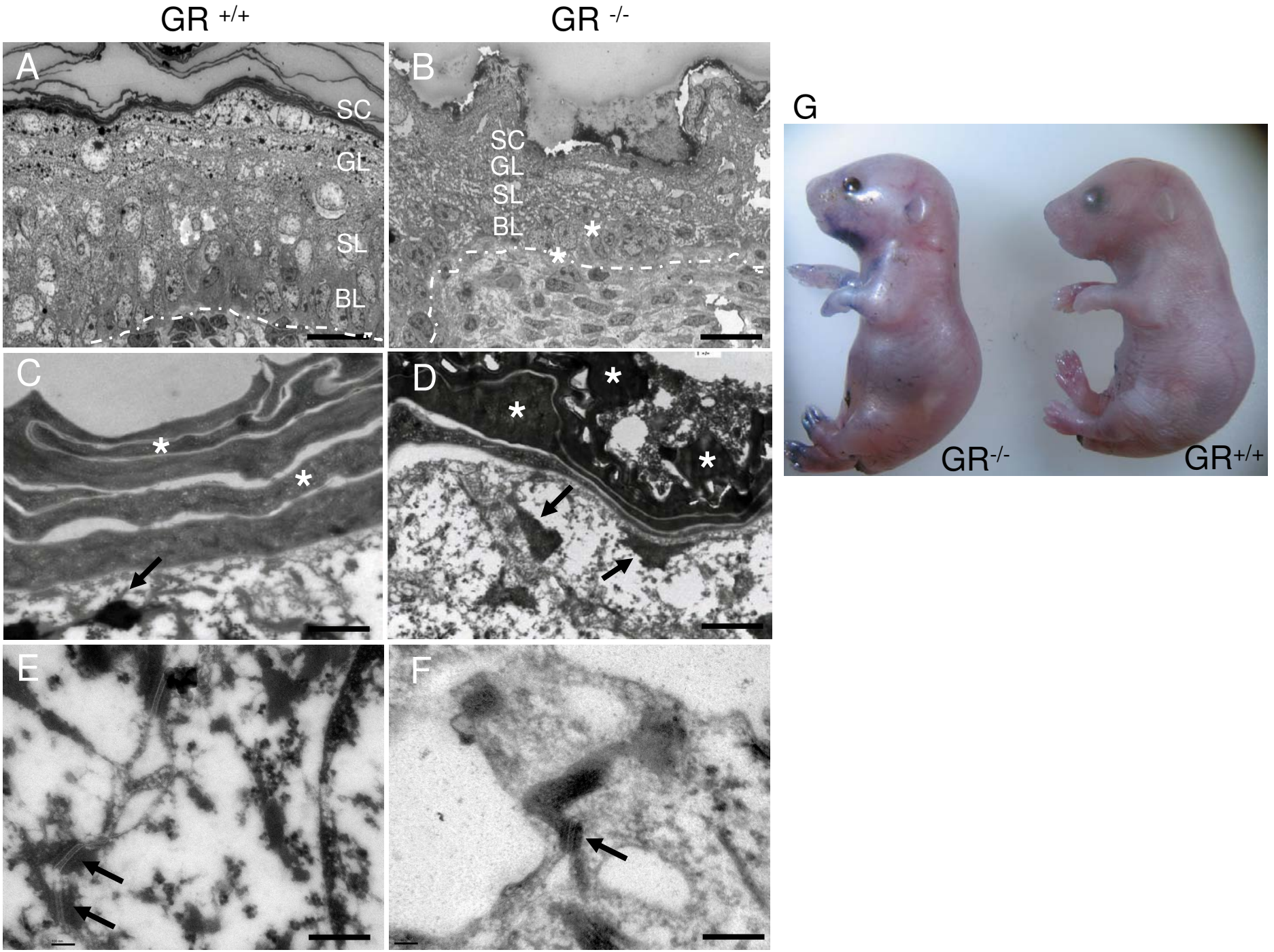
GR +/+
GR -/-
A
SC
GL
SL
BL
B
SC
GL
SL
BL
C
D
E
F
G
GR-/-
GR+/+

Bayo, Fig.4

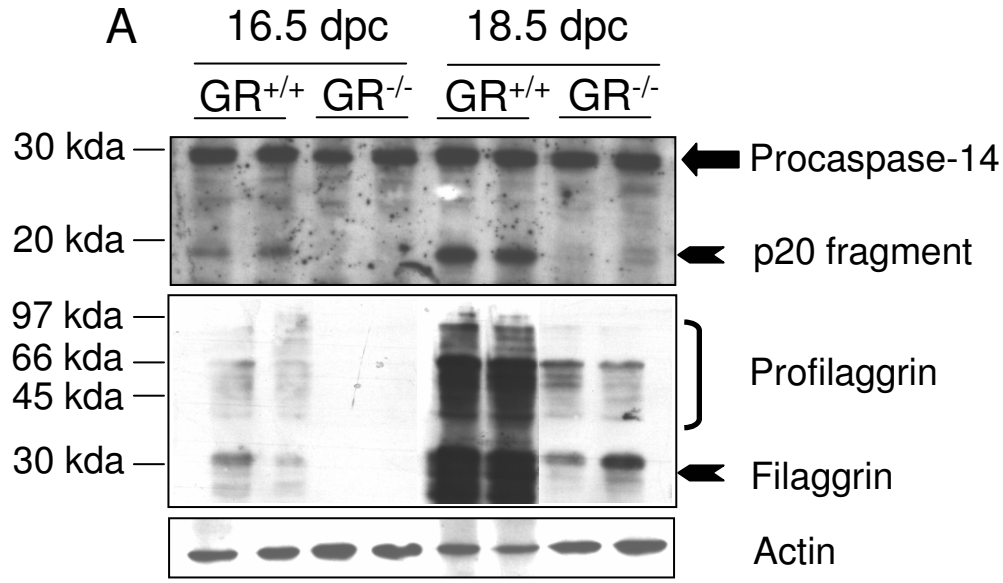
A
16.5 dpc
18.5 dpc
GR+/+ GR-/-
GR+/+ GR-/-
30 kda
20 kda
97 kda
66 kda
45 kda
30 kda
Procaspase-14
p20 fragment
Profilaggrin
Filaggrin
Actin

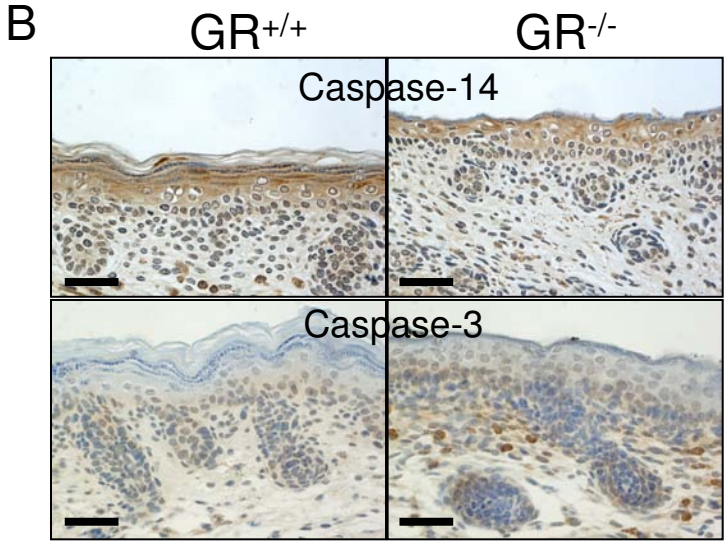
B
GR+/+
GR-/-
Caspase-14
Caspase-3

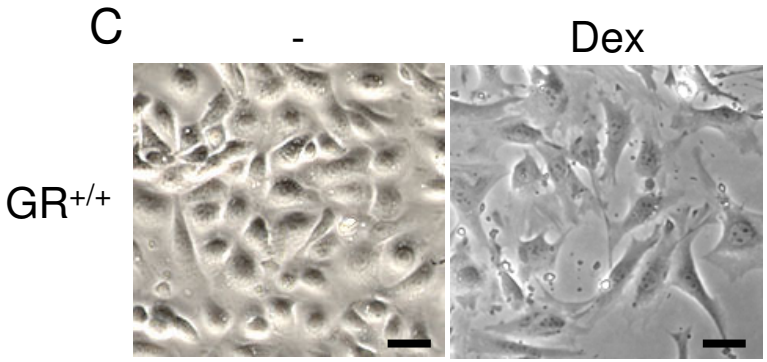
C
-
Dex
GR+/+

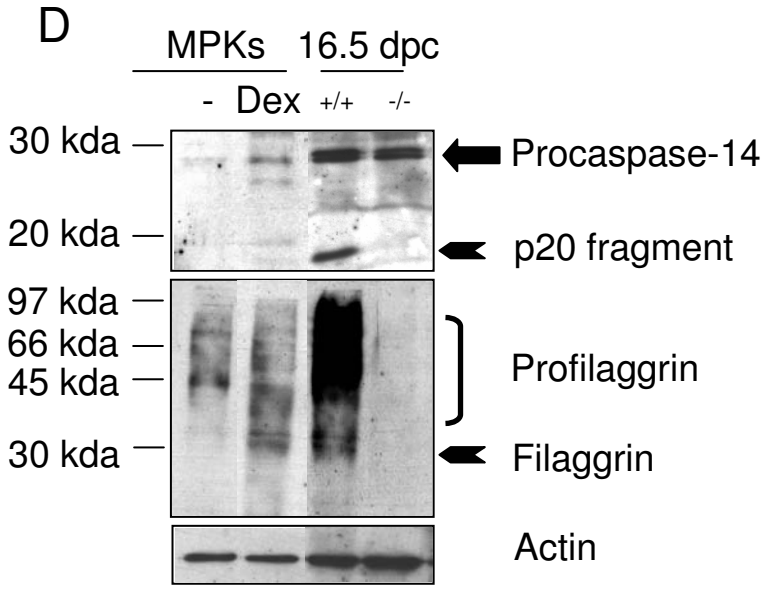
D
MPKs
16.5 dpc
- Dex +/+ -/-
30 kda
20 kda
97 kda
66 kda
45 kda
30 kda
Procaspase-14
p20 fragment
Profilaggrin
Filaggrin
Actin

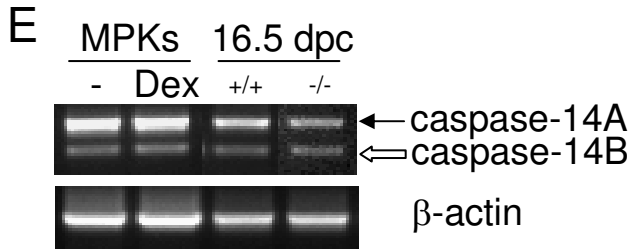
E
MPKs
16.5 dpc
- Dex +/+ -/-
caspase-14A
caspase-14B
β-actin

Bayo, Fig.5

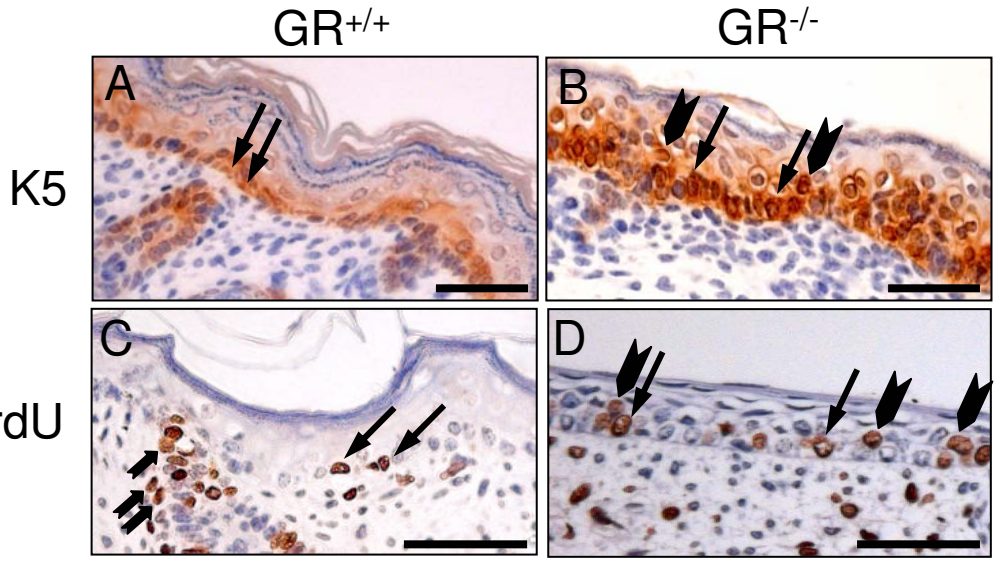
GR+/+
GR-/-
A
B
K5
C
D
BrdU

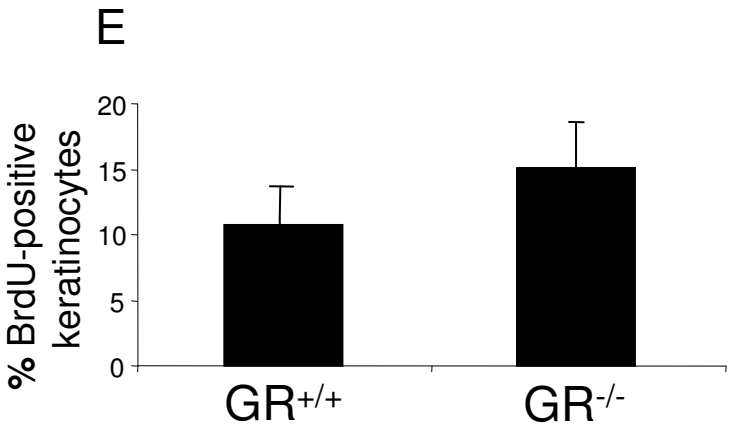
E
% BrdU-positive keratinocytes
20
15
10
5
0
GR+/+
GR-/-

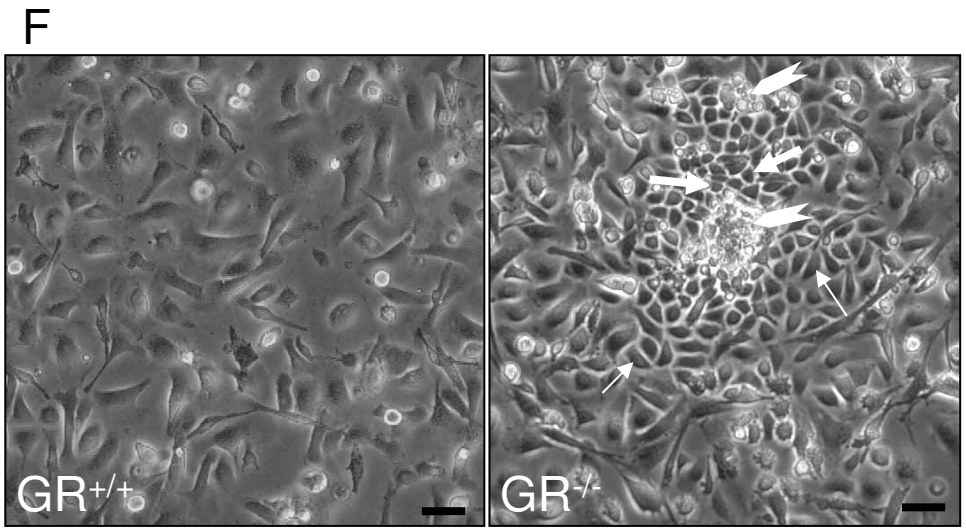
F
GR+/+
GR-/-

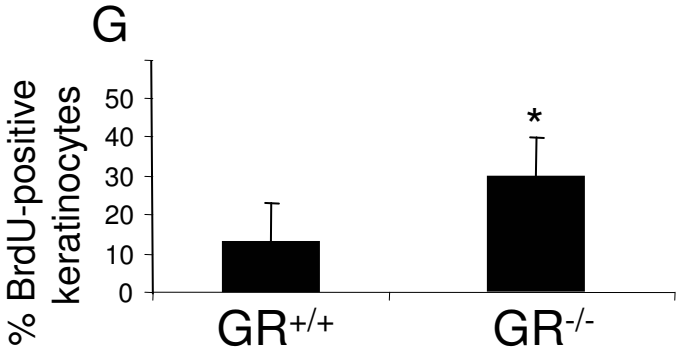
G
% BrdU-positive keratinocytes
50
40
30
20
10
0
*
GR+/+
GR-/-

Bayo, Fig.6

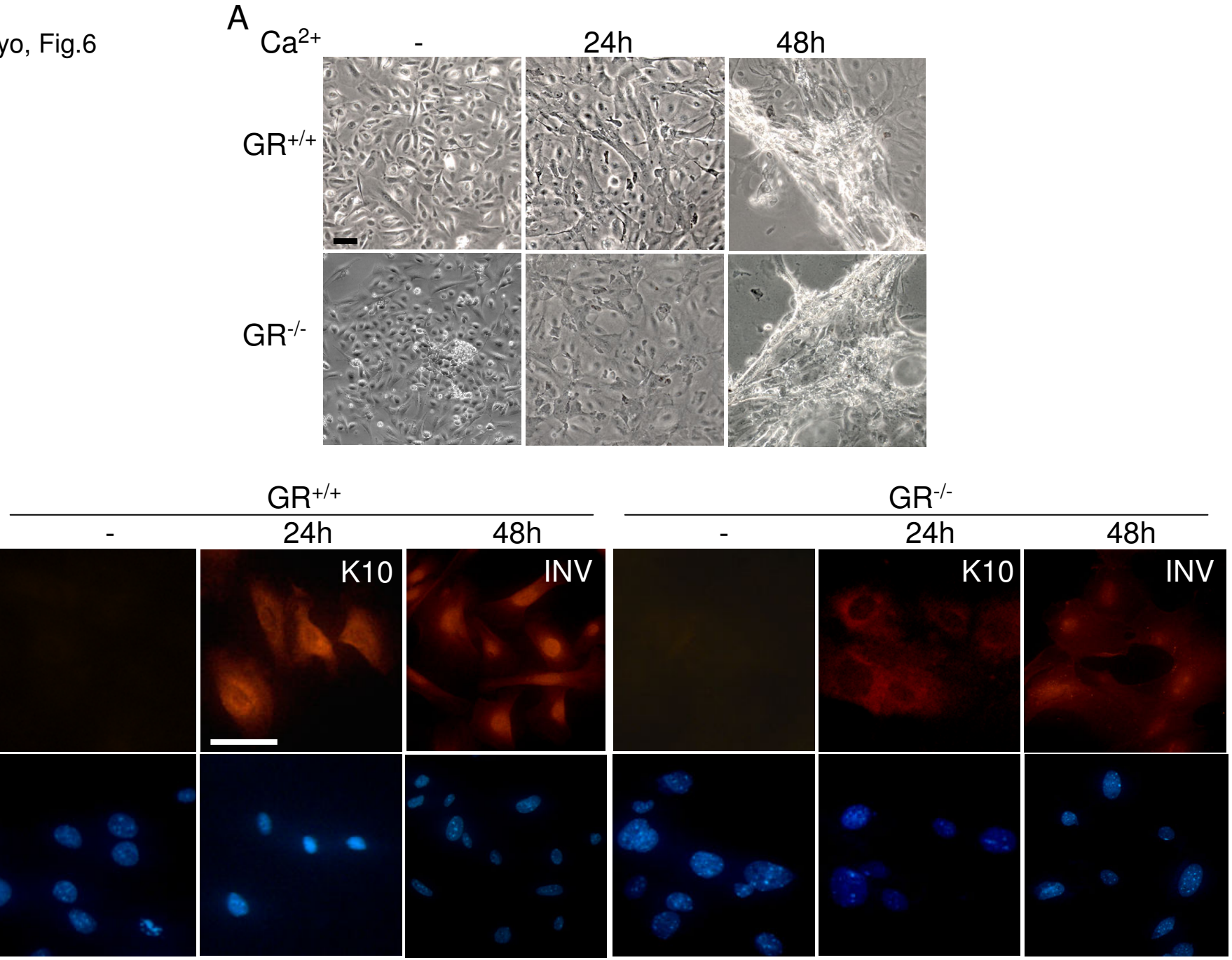

Bayo, Fig.7

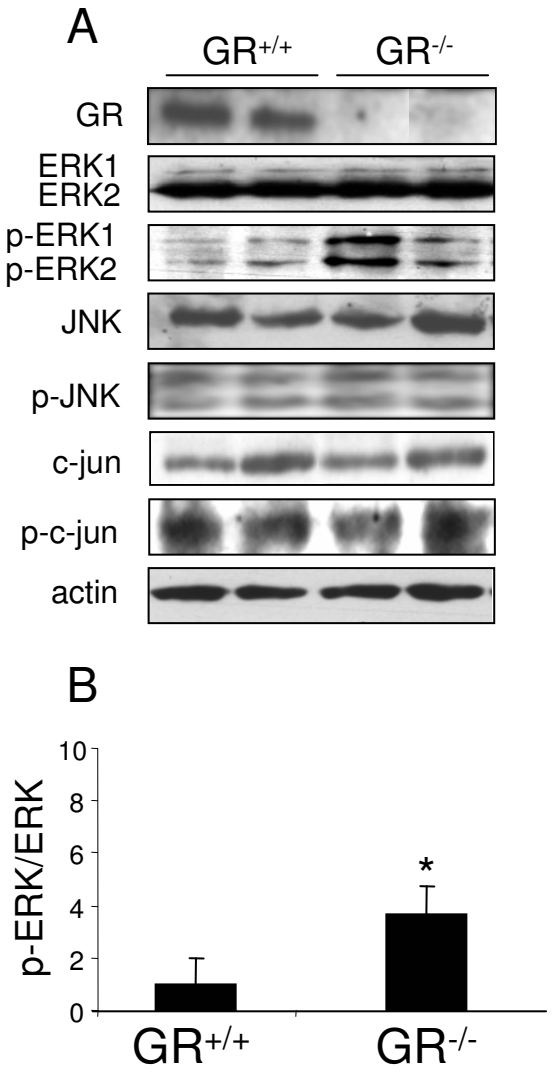
A
GR+/+
GR-/-
GR
ERK1
ERK2
p-ERK1
p-ERK2
JNK
p-JNK
c-jun
p-c-jun
actin
B
p-ERK/ERK
10
8
6
4
2
0
*
GR+/+
GR-/-

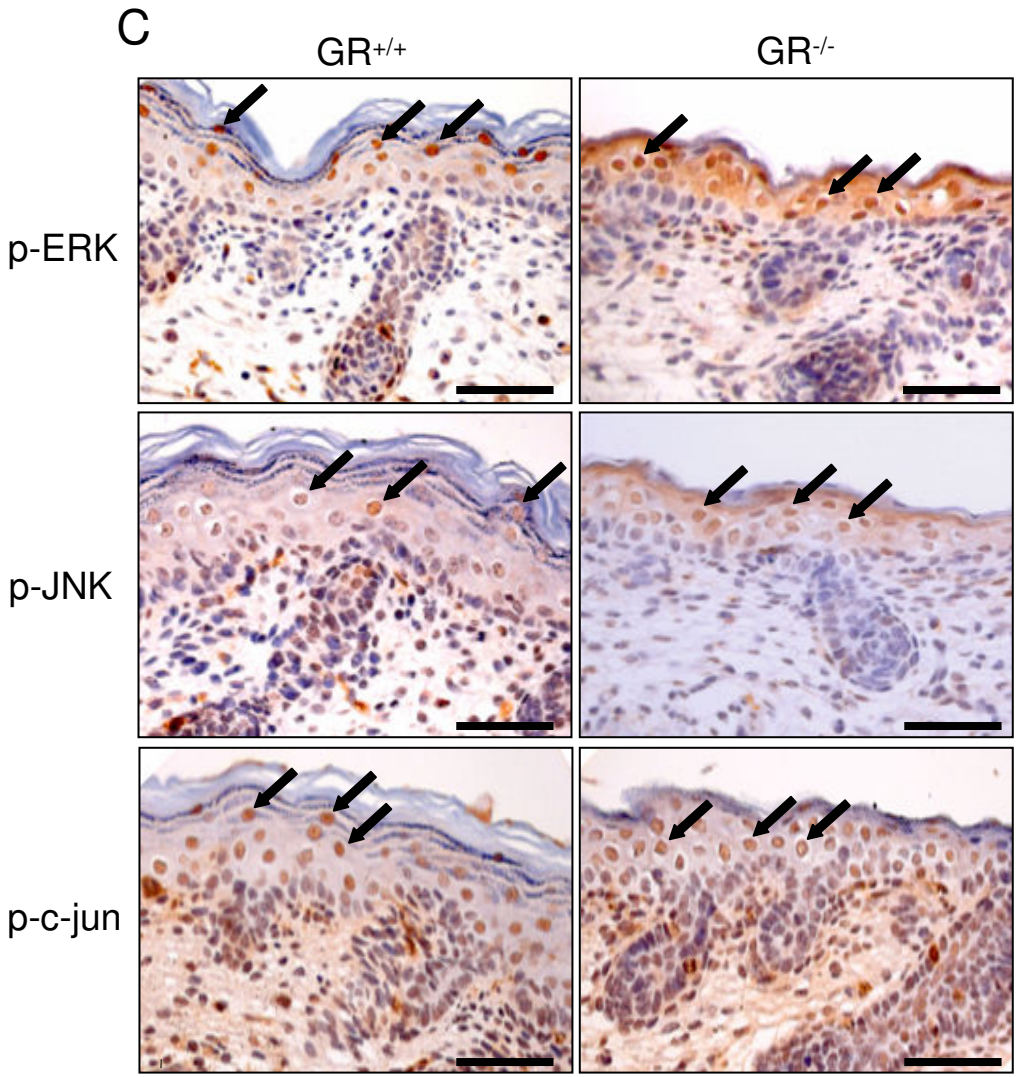
C
GR+/+
GR-/-
p-ERK
p-JNK
p-c-jun

Bayo, Fig.8

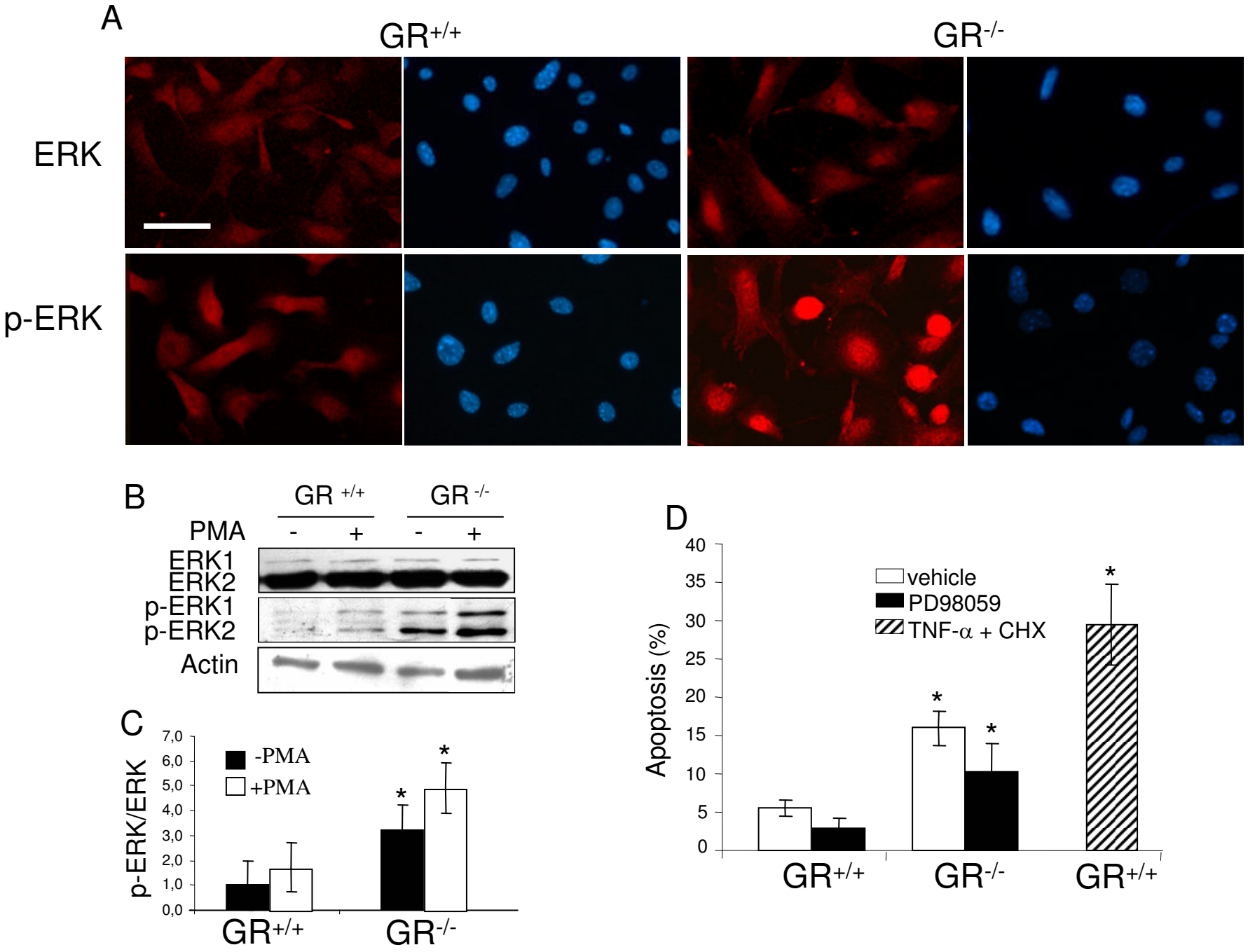
A
GR+/+
GR-/-
ERK
p-ERK
B
GR +/+
GR -/-
PMA
- + - +
ERK1
ERK2
p-ERK1
p-ERK2
Actin
C
p-ERK/ERK
7,0
6,0
5,0
4,0
3,0
2,0
1,0
0,0
-PMA
+PMA
*
*
GR+/+
GR-/-
D
Apoptosis (%)
40
35
30
25
20
15
10
5
0
vehicle
PD98059
TNF-α + CHX
*
*
*
GR+/+
GR-/-
GR+/+

Bayo, Fig.9